Progress In Electromagnetics Research Letters, Vol. 41, 167–174, 2013

DESIGN OF DUAL BAND FILTER BASED ON A NOVEL DGS STRUCTURE

Yang Li*, Hong-Chun Yang, and Shao-Qiu Xiao

School of Physical Electronics, University of Electronic Science and Technology of China, Chengdu 610054, China

Abstract—This letter presents a dual-band bandpass filter (BPF) using interdigital coupling lines with a new defected ground structure (DGS) pattern. Traditional DGS structures are mainly used to realize wide bandstop characteristics. In this letter, by introducing a pair of coupling stubs in the aperture of the DGS, a narrow passband can be achieved within a wide stopband, so a dual-band bandpass filter can be implemented. An equivalent circuit model is derived to describe the filter. And the circuit simulation result agrees well with the EM simulation one. The position and bandwidth of the two passbands can be designed and adjusted independently. In order to verify the theory, a dual-band bandpass filter is designed, fabricated and measured. The simulated and measured results are in good agreement.

1. INTRODUCTION

There has been growing interest in wireless communication systems operating in multi-bands. Dual-band bandpass filters especially have attracted many researchers. References [1, 2] outline the direct design methods for a dual-band band pass filter. In [1], two filters operating at different frequency bands are combined with common input/output ports. In [2], transmission zeros are used to separate the single-passband filter into a dual-passband. However, these methods increase the complexity of the filter design process and the overall size of a filter circuit.

Defected ground structure (DGS) is a kind of transmission line combined with periodic or non-periodic apertures etched in the ground plane. Because of the bandgap and slow wave characteristics, DGS is

Received 15 June 2013, Accepted 20 July 2013, Scheduled 30 July 2013

* Corresponding author: Yang Li (liyang8311@gmail.com).

usually used in lowpass filters [3]. Bandpass filters are composed of cascaded lowpass and highpass filters [4], or used to suppress higher order harmonics in lowpass or bandpass filters [5].

In this letter, a novel DGS structure is proposed. Firstly a traditional DGS with interdigital coupling lines structure (i.e., filter A) is designed to achieve a single passband and wide stopband characteristic. Then by introducing a pair of coupling stubs in the aperture of the DGS (i.e., filter B), a narrow passband can be realized in the stopband. Finally, a dual-band bandpass filter is realized by cascading two filters B. The bandwidth and position of the two passbands can be adjusted independently. In order to validate the theory and design procedure, a dual-band bandpass filter with passband 2.85–4.75 GHz and 8.65–8.95 GHz was designed, fabricated and measured. The simulated and measured results are in good agreement.

2. DESIGN PROCEDURE

Figure 1 shows the basic structure of a bandpass filter composed of DGS and an interdigital coupling line. We call it filter A in this letter. This filter has a single passband property because of the lowpass characteristic of the DGS and highpass characteristic of the interdigital

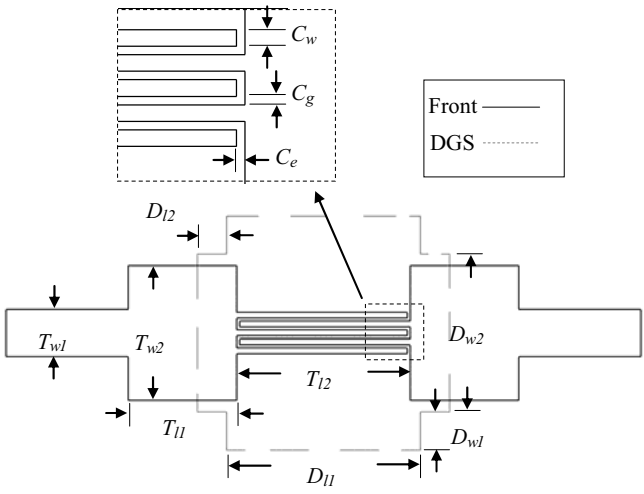

Figure 1. Schematic of a bandpass filter (filter A) comprised of a DGS (dash line) and interdigital coupling lines (solid line) and detailed dimensions of the coupling line.

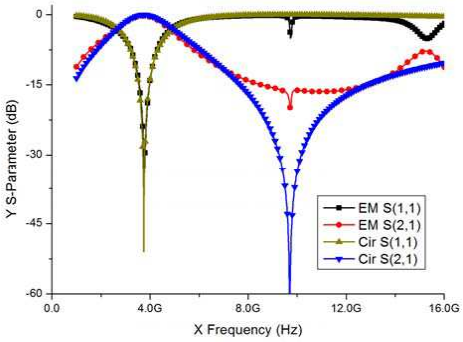

Figure 2. Simulated result of filter A. Associated parameters: $T_{w1} = 1.6$, $T_{w2} = D_{w2} = 4.6$, $T_{l2} = D_{l1} = 5.9$, $D_{w1} = 1.75$, $T_{l1} = 3.7$, $D_{l2} = 1$, $C_w = 0.2$, $C_g = 0.1$, $C_e = 0.1$ (all in millimeters).

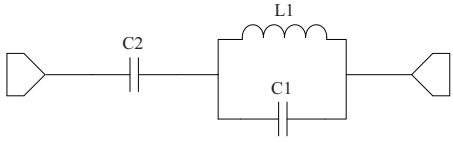

Figure 3. Equivalent circuit of the bandpass filter shown in Fig. 1. $C_2 = 0.32\,\text{pF}$, $C_1 = 0.0561\,\text{pF}$, $L_1 = 4.798\,\text{nH}$.

coupling line. Filter A is simulated using commercial software IE3D. The simulated result is shown in Fig. 2. In the simulation, the substrate used is RT Duroid 5880 with relative permittivity 2.2 and thickness 0.508 mm.

In order to study the filter in a more accurate manner, an equivalent circuit is derived. The topology and parameters of the equivalent circuit are shown in Fig. 3. The circuit parameter extraction method is described below. The defected ground structure can be modeled by a parallel LC resonant circuit. The parameter extraction procedure was described in [6]. The parameters of capacitor C_1 and inductor L_1 of the parallel LC circuit can be calculated by Equations (1) and (2). In these two equations, Z_0 is the terminal impedance, and ω_c and ω_0 denote cut off radian frequency and attenuation pole radian frequency, respectively, which can be obtained from the EM simulation result. The effect of the interdigital coupling line is represented by a series capacitor C_2 in the equivalent circuit. The capacitance can be calculated from Equation (3) [7]. In this equation, l is the length of coupling line and n the number of fingers. The circuit simulation result is depicted in Fig. 2 and compared with

the EM simulated one.

$$C = \frac{\omega_c}{2Z_0} \cdot \frac{1}{\omega_0^2 - \omega_c^2} \tag{1}$$

$$L = \frac{1}{4\pi^2 f_0^2 C} \tag{2}$$

$$C(\text{pF}) = 3.937 \times 10^{-5} l(\varepsilon_r + 1) \cdot [0.11(n-3) + 0.252] + 0.14 \quad (l \text{ in } \mu\text{m}) \tag{3}$$

From the equivalent circuit, it can be discerned that the lower stop frequency of the passband is mainly determined by the capacitance of the interdigitated coupling line and the higher stop frequency mainly determined by the dimensions of DGS. Consequently, the position and bandwidth of passband can be readily tuned by adjusting these parameters.

Figure 4 shows the simulated S_{21} in different situations. Fig. 4(a) displays the trend of S_{21} when increasing the number of coupling fingers of the interdigital line while keeping the DGS dimensions unchanged. Fig. 4(b) plots the S_{21} curves for different widths of DGS while the number of coupling fingers of interdigitated line remains the same. One can notice that when the number of fingers is increased, the lower stop frequency decreases due to the increment of capacitance of C_2 in the equivalent circuit, and at the same time, the higher stop frequency remains essentially unchanged. When the width of DGS is increased, the cut off frequency of the parallel resonant circuit in equivalent circuit decreases, and because C_2 has same value, the lower stop frequency does not change significantly. So the position and bandwidth can be tuned flexibly by changing the capacitance of the interdigital coupling transmission line and dimensions of DGS.

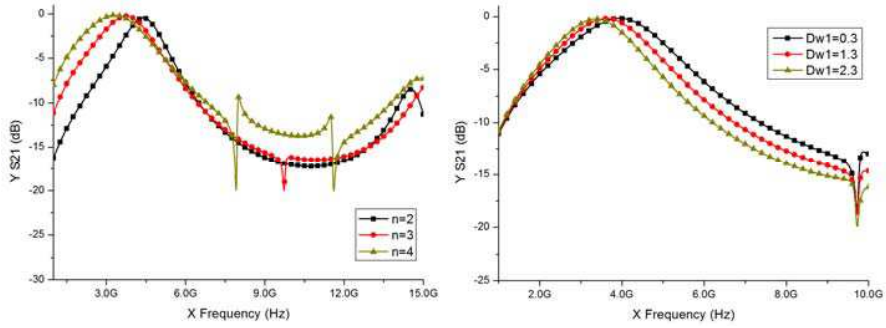

(a) (b)

Figure 4. Simulated S_{21} in different coupling finger numbers and different DGS dimension.

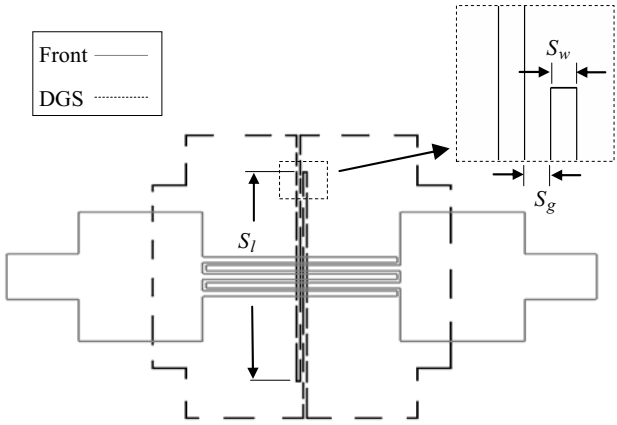

Figure 5. Schematic of filter B and the structure of the modified DGS with a pair of coupling stubs.

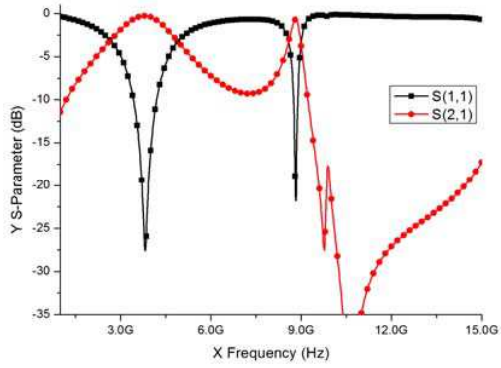

Figure 6. The simulated S-parameters of the filter B. Associated parameters: $S_l = 6.43\,\text{mm}$, $S_w = 0.1\,\text{mm}$, $S_g = 0.1\,\text{mm}$, others are same with those of filter A.

From Fig. 2. It can be seen that the bandpass filter shown in Fig. 1 has a single passband and a wide stopband characteristic. In order to achieve the second passband, a modified DGS pattern can be used, as shown in Fig. 5.

In this structure, a pair of coupling stubs is added in the center of the DGS vertically. The width of one stub is S_w, the gap between two stubs S_g, and the coupling length S_l. The new filter with modified DGS structure is named filter B in this letter. This structure was simulated by IE3D, and the result is shown in Fig. 6.

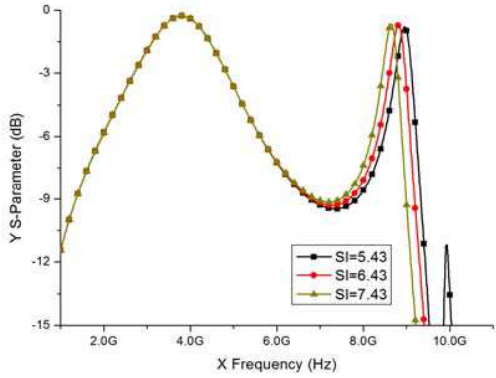

Figure 7. Simulated S_{21} of the dual-band filter with different S_l.

The parameters of the new filter are the same as the one presented in Fig. 1 excluding the coupling stubs.

From the simulation result depicted in Fig. 6, it can be seen that the second passband appears at 8.8 GHz because of a transmission pole introduced by the coupling stubs. The position of the second passband depends on the length of the coupling stubs S_l, so it can be adjusted by changing the length. Fig. 7 shows the simulated S_{21} with different S_l.

3. SIMULATION AND MEASUREMENT RESULTS

In order to verify the design procedure and simulation results shown above, a dual-band bandpass filter formed by cascading by two filters B was designed, fabricated and measured. The schematic is shown in Fig. 8. Only the parameters of the transmission line between the two filter sections are labeled, and other parameter values can be found in Fig. 1 and Fig. 5. A photograph of the fabricated filter is shown in

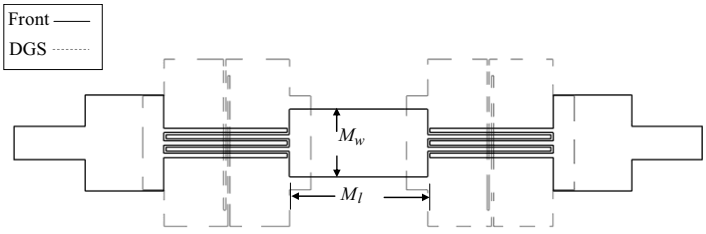

Figure 8. Schematic of the filter cascaded by two filters B.

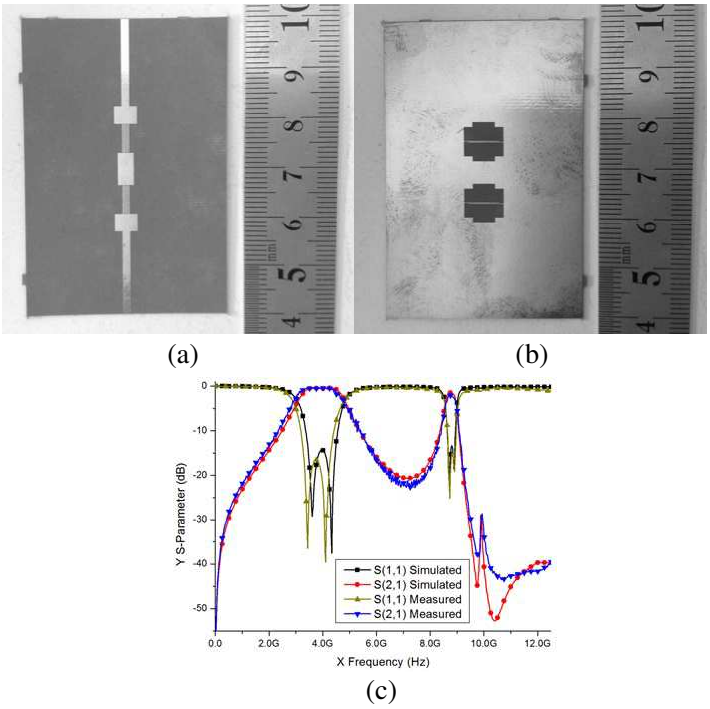

Figure 9. (a) Photograph of front side of the fabricated filter. (b) Back side. (c) Simulated and measured frequency responses of fabricated dual-band BPF.

Fig. 9.

The parameters optimized by IE3D are $T_{w1} = 1.6\,\text{mm}$, $T_{w2} = D_{w2} = 4.6\,\text{mm}$, $T_{l2} = D_{l1} = 5.9\,\text{mm}$, $D_{w1} = 1.75\,\text{mm}$, $T_{l1} = 3.7\,\text{mm}$, $D_{l2} = 1\,\text{mm}$, $C_w = 0.2\,\text{mm}$, $C_g = 0.1\,\text{mm}$, $C_e = 0.1\,\text{mm}$, $S_l = 6.43\,\text{mm}$, $S_w = 0.1\,\text{mm}$, $S_g = 0.1\,\text{mm}$, $M_w = 3.2\,\text{mm}$, $M_l = 6.5\,\text{mm}$. The substrate used has a relative dielectric constant of 2.2 and thickness 0.508 mm. Furthermore, the size of the filter can be made more compact by truncating the size of the ground plane without significant effect. Fig. 9(c) is the simulated and measured results of the proposed dual-band BPF, and good agreement between them is observed. The 3 dB passband covers the range of 2.85–4.75 GHz and 8.65–8.95 GHz. The minimum insertion loss is $-0.4\,\text{dB}$ while the maximum return loss is $-16\,\text{dB}$ within the first passband. Likewise, within the second passband, the minimum insertion loss is $-1.7\,\text{dB}$ while the maximum return loss is $-15\,\text{dB}$.

4. CONCLUSIONS

A novel structure is developed for the dual-passband BPF in this letter. By introducing a pair of coupling stubs in the aperture of DGS, a second passband can be achieved. The bandwidth and position of the two passband can be adjusted independently. In order to verify the simulation result, a prototype BPF was fabricated and measured. The measured and simulated results are in good agreement.

ACKNOWLEDGMENT

This work was supported by the Fundamental Research Funds for the Central Universities.

REFERENCES

1. Chen, C.-Y. and C.-Y. Hsu, "A simple and effective method for microstrip dual-band filters design," *IEEE Microw. Wirel. Compon. Lett.*, Vol. 16, No. 5, 246–248, 2006.
2. Quendo, C., E. Rius, and C. Person, "An original topology of dual-band filter with transmission zeros," *IEEE MTT-S Int. Microw. Symp. Dig.*, 1093–1096, 2003.
3. Lim, J.-S., C.-S. Kim, et al., "Design of low-pass filters using defected ground structure," *IEEE Transactions on Microwave Theory and Techniques*, Vol. 53, No. 8, 2539–2545, 2005.
4. Yang, G. M., R. Jin, et al., "Ultra-wideband bandpass filter with hybrid quasi-lumped elements and defected ground structure," *IET Microwaves, Antennas & Propagation*, Vol. 1, No. 3, 733–736, June 2007.
5. Ting, S.-W., K.-W. Tam, et al., "Miniaturized microstrip lowpass filter with wide stopband using double equilateral U-shaped defected ground structure," *IEEE Microw. Wirel. Compon. Lett.*, Vol. 16, No. 5, 240–242, 2006.
6. Ahn, D., J. S. Park, et al., "A design of the low-pass filter using the novel microstrip defected ground structure," *IEEE Transactions on Microwave Theory and Techniques*, Vol. 49, No. 1, 86–93, 2001.
7. Hong, J. S. and M. J. Lancaster, *Microstrip Filters for RF/Microwave Applications*, John Wiley, New York, 2001.